Effect of Solid Carriers on Oxygen Mass Transfer in a Stirred Tank Bioreactor

TANASE DOBRE, BRINDUSA SANDU OHREAC, OANA CRISTINA PARVULESCU*, TIBERIU DINU DANCIU
Politehnica University of Bucharest, Chemical and Biochemical Engineering Department, 1-3 Gheorghe Polizu, 011061, Bucharest, Romania

Various strategies for improving the mass transfer rate of oxygen have been used in order to obtain a good efficiency of aerobic fermentation processes. The paper focuses on studies concerning the influence of solid carrier addition in the liquid phase on oxygen volumetric mass transfer coefficient in a stirred and aerated tank bioreactor. The selected oxygen carriers (vectors) can be easily separated and they have no harmful effect on the microbial population implied in bioprocesses. Fine particle of activated carbon, silicon oil impregnated activated carbon, bacterial cellulose, magnetite, and bacterial cellulose-magnetite composite were used as oxygen-vectors. An enhancement of oxygen transfer was indicated by an increase in volumetric mass transfer coefficient, k_la, which was determined by a dynamic method. A significant improvement of oxygen mass transfer in the presence of magnetite and bacterial cellulose-magnetite composite was highlighted.

Keywords: aerobic biosynthesis, biocellulose composite, magnetite, mass transfer, oxygen-vector, stirred bioreactor

*

A characterization of oxygen mass transfer at the gas-liquid interface is essential to design, scale up and operate the aerobic bioreactors. The oxygen transfer rate is strongly influenced by the bioreactor type, operational conditions, fermentation broth composition, microorganisms type, and concentration. In an aerobic bioprocess, the microbial cells use oxygen for various metabolic processes, especially growth and synthesis of metabolic compounds. In order to obtain an optimal cell growth and an efficient synthesis of the desired metabolites, an accurate prediction of oxygen transfer kinetics is a key step [1-5]. For stirred and aerated tank bioreactors, widely employed in a large variety of bioprocesses, there are manifold data, relationships, and procedures to estimate the oxygen transfer rate [5-10]. Firstly, considering the oxygen diffusion in liquid film surrounding the air bubble as rate-determining step, the transfer rate is proportional to the partial volumetric mass transfer coefficient, k_la, which depends on the stirring speed, aeration system, air flow rate, medium homogeneity, fermentation broth composition, and microbial cells activity. On the other hand, the transfer rate is determined by the transfer driving force expressed as difference between oxygen concentration at gas-liquid interface and oxygen concentration in bulk liquid. The oxygen concentration at gas-liquid interface (usually ranging from 3 to 10 mg/L) depends on its solubility, which is commonly determined by temperature, pressure, and fermentation broth composition [11,12].

Lately, a special attention is paid to addition of oxygen-vectors in culture medium in order to promote the oxygen transfer in stirred aerobic bioreactors. An oxygen-vector is a compound which can enhance the oxygen transfer rate, either due to its ability to augment the oxygen solubility in fermentation medium leading to an increase in driving force or to enlarge the gas-liquid interfacial surface area yielding an improvement of volumetric mass transfer coefficient, k_la. The most common oxygen-vectors used in biotechnology are liquids, e.g. hydrocarbons, perfluorocarbons, synthetic (silicone) oils, and vegetable oils (palm, olive, soybean, castor), which are non miscible with water, the main constituent of the fermentation broth [13-18]. The solubility of oxygen in these liquid vectors is about 10 times larger than its solubility in water, causing a Marangoni effect at the gas-liquid interface. Accordingly, they determine an increase in oxygen transfer driving force by oxygen solubility rising as well as an increase in liquid phase partial mass transfer coefficient as effect of interfacial Marangoni instabilities.

Studies in the related literature assessed an enhancement of gas-liquid mass transfer in the presence of some bulk solid materials [19,20]. Moreover, the solids can be easily separated from medium. The idea to test solid compounds as potential oxygen-vectors in aerobic biosynthesis was based on these two considerations. According to the surface renewal theory (Dankwerts) in the interphase mass transfer, it can be realistic an action mechanism as follows: i) an air bubble comes into contact with a solid particle, ii) oxygen molecules are transferred through the bubble surface and are adsorbed onto the solid, iii) the solid particle is dislodged from the contact surface and diffuses into the liquid, iv) oxygen molecules are desorbed and released in the liquid phase.

The paper has aimed at testing some solid materials as oxygen-vectors in a stirred and aerated tank bioreactor as well as at establishing the dependence of oxygen volumetric mass transfer coefficient, k_la, on liquid phase composition, stirring and aeration conditions. A batch phases contacting and a dynamic method based on oxygen degassing and re-aeration were selected for experimental determination of k_la. In the degassing stage, the oxygen was removed from liquid phase, consisting of either water or aqueous solution containing a solid oxygen-vector, whereas in the re-aeration stage, compressed air was supplied till the concentration of dissolved oxygen (DO) in liquid phase, c_l, reached a constant value, c_l^*, indicating an equilibrium state. Experimental curves describing the time variation of DO concentration, $c_l(\tau)$, at constant temperature (DO curves), obtained by air contacting with

* email: oana.parvulescu@yahoo.com; Tel.: (+40) 021 402 38 10

water and aqueous solutions containing various solid oxygen-vectors, i.e. fine particles of activated carbon, silicon oil impregnated activated carbon, bacterial cellulose, magnetite, and bacterial cellulose-magnetite composite, have been reported.

The oxygen volumetric mass transfer coefficient, k_la, can be estimated based on experimental DO curves according to characteristic equation (1) of dynamic method [1-20]. The correlation (2), a particular form of equation (1) for two points on a DO curve, was used to determine the value of k_la in two-phase (air-water) and three-phase (air-water-solid vector) systems.

$$\ln\left(1-\frac{c_l}{c_l^*}\right)=-k_l a\,\tau \quad (1)$$

$$k_l a=\frac{1}{(\tau_2-\tau_1)}\ln\left(\frac{c_l^*-c_{l1}}{c_l^*-c_{l2}}\right) \quad (2)$$

Experimental part

Materials and methods

Compressed air was used as phase containing oxygen whereas the liquid medium in bioreactor consisted of water as well as of aqueous solutions containing various amounts of oxygen-vector. As solid oxygen-vectors were employed activated carbon (AC), fine particles of silicon oil impregnated activated carbon (AC-SO), magnetite (MG) powder, finely ground membranes of bacterial cellulose (BC), and bacterial cellulose-magnetite (BC-MG) composite.

Activated carbon (AC) was supplied by Carlo Erba Reagents with the following characteristics: 350±50 kg/m^3 apparent density, min. 1000 m^2/g BET specific surface, max. 0.1 % iron content, max. 0.05 mm particle mean diameter (Carlo Erba code 08.52.12.100). In order to prepare a silicon oil impregnated activated carbon (AC-SO), an amount of 100 g activated carbon was vigorously mixed with 15 g of silicone oil provided by Sigma-Aldrich Corporation (Fluka Chemicals Silicon DC-200 code 85377). The hardened mixture obtained by impregnation was kept for 24 h under nitrogen atmosphere and then crushed in fine particles.

Bacterial cellulose (BC) membranes were synthesized in laboratory according to the procedures described in our previous papers [21,22]. In order to prepare a bacterial cellulose-magnetite (BC-MG) composite as well as magnetite (MG) particles, two solutions were prepared, the former containing 0.03 M $FeSO_4 \cdot 6H_2O$ and the latter 0.02 M $FeCl_3$. The solutions were mixed for 30 minutes under nitrogen atmosphere and vigorous mechanical stirring (about 600 rpm). A BC membrane (M1) was added in this well mixed solution containing Fe^{+2} and Fe^{+3} and kept at 50°C for 30 min under nitrogen atmosphere and magnetic stirring. The membrane extracted from the solution after 30 min was then immersed in 100 mL of 0.3 M sodium hydroxide solution. A dark brown precipitate was instantaneously formed on the M1 membrane surface. Another BC membrane (M2) was immersed in the solution containing Fe^{+2} and Fe^{+3} and kept at 50°C for 30 min under nitrogen atmosphere and magnetic stirring. An amount of 300 mL of 0.3 M sodium hydroxide solution was added by drip under agitation into the solution containing the M2 membrane. A black precipitate was instant-aneously formed on the M2 membrane surface. Both M1 and M2 composite membranes were repeatedly washed with water till a *p*H of 7 was obtained in the washing solution. Fine particles of magnetite (MG), Fe_3O_4, less 40 μm diameter, were obtained by decantation and magnetic separation of sodium hydroxide solutions. Both BC-MG composite membranes and MG particles were further dried out in a heating oven at 50°C. The same procedures were repeated using another two BC membranes, i.e. M3 and M4, but raising the temperature of solution containing Fe^{+2} and Fe^{+3} from 50 to 80°C. The membranes of BC-MG composite and those of BC were finely ground for their testing as oxygen-vectors.

Equipment and procedure

The experiments were conducted in a stirred tank bioreactor (Biostat Aplus Sartorius), 2 L working volume and D=0.15 m glass tank diameter. The parameters recorded by a computer attached to the bioreactor were temperature, liquid level, *p*H, and pO_2. The homogenization of the medium in the bioreactor was accomplished by mechanical stirring by means of a six-blade disk impeller (Rushton), d=0.052 m diameter, h=0.03 m distance between stirrer inferior part and tank bottom. Vertical baffles were inserted to assist the medium homogenization. The bioreactor was equipped with an air micro-sparger system in order to obtain well dispersed small air bubbles and, consequently, a better gas-liquid contact.

The volumetric mass transfer coefficient, k_la, was estimated using a dynamic method consisting of two stages, i.e. degassing and re-aeration. In the degassing stage, the oxygen was removed from liquid phase by a stream of nitrogen which was fed till the level of dissolved oxygen reached a minimum value very close to 0. In the re-aeration stage, compressed air was supplied through the micro-sparger system till the concentration of dissolved oxygen in liquid phase attained a constant value, indicating an interphase equilibrium state.

The crystalline structure of BC-MG composite was analyzed based on characteristic measurements of scanning electron microscopy (SEM), energy dispersive X-ray spectroscopy (EDX), and X-ray diffraction (XRD).

Operational conditions

The experiments were performed at a temperature t=30°C, a liquid phase volume V=1 L, and a liquid level H=0.057 m, respectively. In the degassing stage, the nitrogen was supplied at a constant volumetric flow rate G_{vn}=2 L/min, determining a dynamic nitrogen intake $c_{dn}=G_{vn}/V=2$ min^{-1}. Selected values of air volumetric flow rate, G_{va}, in the re-aeration stage were 0.5 L/min^{-1}, 1 L/min^{-1}, and 1.5 L/min, resulting a dynamic air intake, $c_{da}=G_{va}/V$, of 0.5 min^{-1}, 1 min^{-1}, and 1.5 min^{-1}, respectively.

Experimental study was conducted at three levels of process independent variables (factors), i.e. concentration of oxygen-vector in water, c_{ov}, stirring speed, n, and dynamic air intake, c_{da}. Six experimental sets including 135 of experiments were carried out according to data summarized in table 1. Additionally, two sets of 9 experiments were performed at a concentration of MG and BC-MG composite, respectively, of 0.15%. The content of dissolved oxygen (DO) was continuously measured by a pO_2 transducer.

Results and discussions

Characterization of BC-MG composite structure

SEM images in figure 1 emphasize the deposition of magnetite (MG), Fe_3O_4, on the bacterial cellulose (BC) fibrils. Comparing characteristic images of composite based on M1 and M3 membranes, it is obvious that a larger MG amount is deposed on the BC fibrils of M3 composite

Aqueous solution	c_{ov} (%)			n (rpm)			c_{da} (min^{-1})			Experimental set	Experiments number
Water	0	0	0	250	500	800	0.5	1	1.5	1	3^2=9
Water-BC	0.3	0.5	0.7							2	3^3=27
Water-AC	0.5	1.0	3.0							3	3^3=27
Water-(AC-SO)	1.0	2.0	-							4	$2 \cdot 3^2$=18
Water-MG	0.3	0.5	1.0							5	3^3=27
Water-(BC-MG)	0.3	0.5	0.7							6	3^3=27

Table 1
PROCESS FACTORS LEVELS

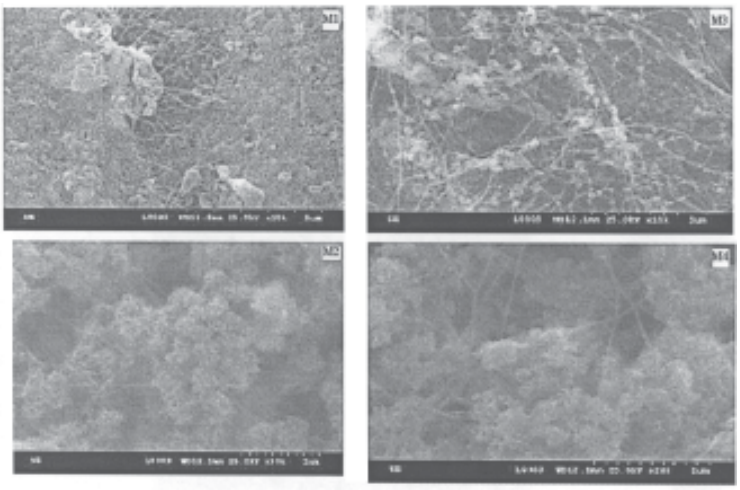

Fig. 1. SEM images of BC-MG composite

membrane, which was synthesized at a higher temperature. Images of M2 and M4 composite membranes highlight an agglomeration of MG particles in a cluster form as well as a larger MG amount than in the composite based on M1 and M3 membranes. Structural differences between M1 and M2 as well as between M3 and M4 composite membranes are due to the differences in their preparation procedure. All MG particles shown in figure 1 present characteristic dimensions of nanoparticles.

EDX pattern of BC (M4)-MG composite (fig. 2) highlights two signals for Fe, indicating the presence of a small amount of Fe_2O_3 besides Fe_3O_4 deposed on BC fibrils. Moreover, a uniform distribution of Fe_3O_4 in composite structure and the existence of other compounds, especially Ca compounds, are proved by the graphic representations in figure 2.

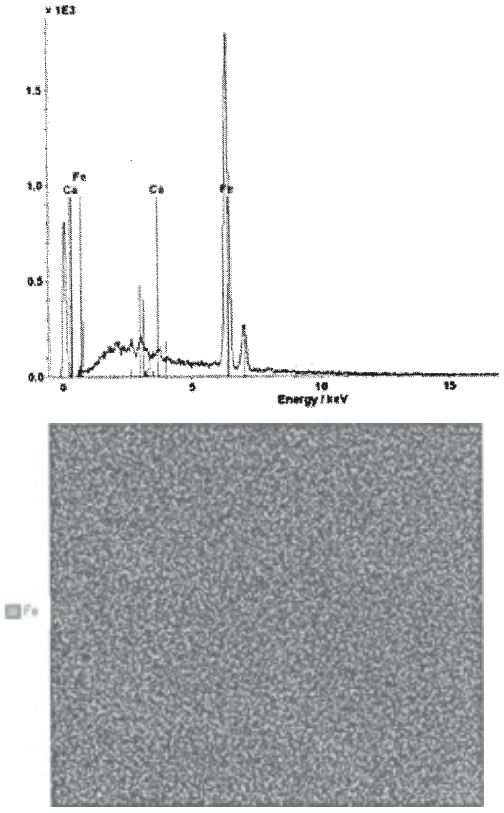

Fig. 2. EDX analysis results for BC (M4)-MG composite

Bacterial cellulose, magnetite, and calcite were identified as crystallized structures by XRD analysis, as shown XRD pattern for BC (M4)-MG composite (fig. 3). The pattern depicted in figure 3 reveals also a large dispersion characterizing the dimension of MG particle.

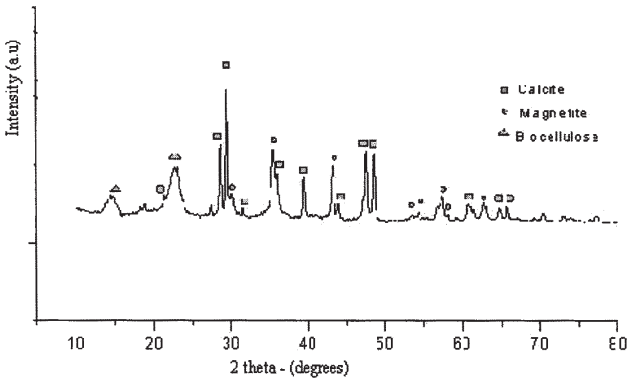

Fig. 3. XRD pattern for BC (M4)-MG composite

Estimation of volumetric mass transfer coefficient, k_la, in bioreactor aqueous phase

The characterization of oxygen mass transfer was accomplished by establishing the dependence of volumetric mass transfer coefficient, k_la, on process factors, i.e. concentration of oxygen-vector in water, c_{ov}, stirring speed, n, and dynamic air intake, c_{da}. The qualitative analysis of the hydrodynamic behaviour of solid oxygen-vectors in the bioreactor tank at low values of stirring speed highlighted a tendency of solid carriers to settle down and, consequently, an inhomogeneous medium structure. An increase in stirring speed as well as in air flow rate led to an improvement of solid dispersion. Well dispersed small oxygen bubbles were obtained due to a better solid dispersion which could determine an enhancement of oxygen mass transfer by an increase in transfer surface area. A quantitative dependence $k_la=k_la\ (c_{ov}, n, c_{da})$ was obtained based on experimental curves describing the dynamics of oxygen concentration in liquid phase, $c_l(\tau)$, obtained for various aqueous phase compositions, mixing and aeration conditions. The values of equilibrium oxygen

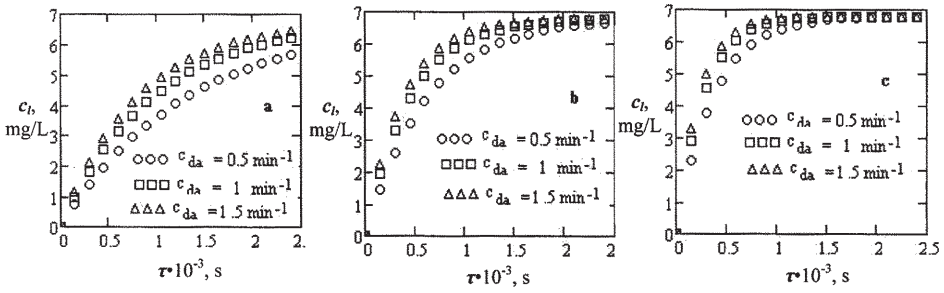

Fig. 4. Dynamics of water oxygenation in Biostat Aplus bioreactor (V=1 L, t=30°C): a) n=250 rpm; b) n=500 rpm; c) n=800 rpm.

Table 2
ESTIMATED VALUES OF k_la DEPENDING ON n AND c_{da} FOR EXPERIMENTAL SET 1

k_la (s^{-1})	n=250 rpm	n=500 rpm	n=800 rpm
c_{da}=0.5 min^{-1}	0.00075	0.00161	0.00269
c_{da}=1.0 min^{-1}	0.00102	0.00219	0.00368
c_{da}=1.5 min^{-1}	0.00123	0.00263	0.00442

concentration in liquid phase, c_l^*, and mass transfer coefficient, k_la, were identified for each experimental oxygenation curve depicted in figures 4, 6-10.

Experimental set 1 (aqueous phase: water)

Figure 4 presents characteristic experimental curves of water oxygenation in bioreactor at various levels of stirring and aeration rate. A value c_l^*=6.8 mg/L of equilibrium oxygen concentration in liquid phase was identified based on experimental data. Moreover, it is observed that the both factors influence the oxygenation dynamics, i.e. the process rate is larger and the saturation is reached faster at higher levels of n and c_{da}. The values of k_la, estimated using the equation (2) for each characteristic oxygenation curve of experimental set 1, are summarized in table 2. The variation of volumetric mass transfer coefficient depending on stirring and aeration conditions is shown in figure 5, which was obtained based on *regress*, *interp*, and *create mesh* functions in Mathcad. Data in table 2 and figure 5 emphasize a significant increase of k_la with stirring speed, whereas the influence of aeration rate is less important.

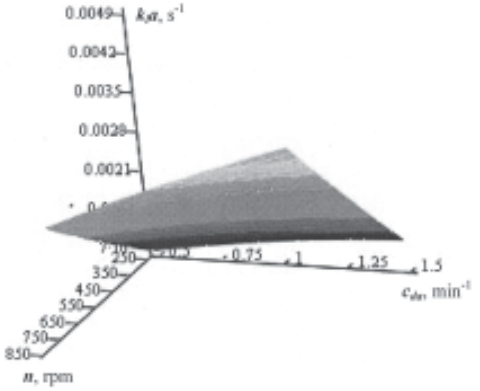

Fig. 5. Dependence of k_la on n and c_{da} for water oxygenation

Table 3 contains the data listed in table 2 expressed in dimensionless form as similitude criteria defined by equations system (3). Sherwood number, *Sh*, depends on partial volumetric mass transfer coefficient of oxygen in liquid phase, k_la, stirrer diameter, d, and diffusion coefficient of oxygen in liquid phase, D_{ol}. Reynolds number, *Re*, is expressed depending on stirring speed, n, stirrer diameter, d, liquid density, ρ_l, and viscosity, η_l. Modified Weber number, We_m, is determined by dynamic air intake, c_{da}, tank diameter, D, liquid viscosity, η_l, and surface tension, σ. The results summarized in table 3 correspond to constant values of geometric simplexes, i.e. D/d=3, H/d=2, h/d=0.6.

$$\begin{cases} Sh = \dfrac{k_l a d^2}{D_{ol}} \\ \mathrm{Re} = \dfrac{n d^2 \rho_l}{\eta_l} \\ We_m = \dfrac{\eta_l D c_{da}}{\sigma} \end{cases} \quad (3)$$

Experimental set 2 (aqueous phase: water-BC)

Characteristic experimental curves of water-bacterial cellulose (BC) oxygenation in bioreactor at various levels of process factors are depicted in figure 6. It is observed that the process dynamics follows a very similar trend to that corresponding to water oxygenation. Moreover, the same value of equilibrium oxygen concentration in liquid phase, i.e. c_l^*=6.8 mg/L, was identified at each value of BC concentration in water, c_{BC}. Referring to the oxygen mass transfer rate, data presented in figure 6 and table 4 reveal a very slight decrease with BC concentration increasing, probably due to an increase in liquid phase viscosity. Thus, estimating the liquid phase viscosity at 30°C using Einstein equation (4), where Φ is solid volume fraction and η_{l0}=0.00081 kg/ms represents water viscosity, the results obtained are as follows:$\eta_{l,0.3\%}$=0.00091 kg/ms, $\eta_{l,0.5\%}$=0.00102 kg/ms, and $\eta_{l,0.7\%}$=0.00115 kg/ms.

$$\eta_l = \eta_{l0}(1 + 2.5\phi) \quad (4)$$

Data listed in table 4 emphasize an increasing variation of *Sh* number with *Re* and We_m numbers, meaning an increase in k_la with n and c_{da} increasing. Similar to water oxygenation, this effect is significant for n and *Re* number, respectively.

Experimental set 3 (aqueous phase: water-AC)

Results concerning the water-activated carbon (AC) oxygenation, which are presented in figure 7 and table 5, highlight two aspects: i) values for k_la and *Sh* number, respectively, very close to those obtained for water and

Table 3
DEPENDENCE OF *Sh* ON *Re* AND We_m FOR WATER OXYGENATION IN BIOSTAT APLUS BIOREACTOR (t=30°C, D/d=3, H/d=2, h/d=0.6)

Sh	*Re*=1.259•10^4	*Re*=2.518•10^4	*Re*=4.029•10^4
We_m=1.422•10^{-5}	1.25•10^3	2.683•10^3	4.483•10^3
We_m=2.844•10^{-5}	1.71•10^3	3.651•10^3	6.133•10^3
We_m=4.266•10^{-5}	2.05•10^3	4.383•10^3	7.367•10^3

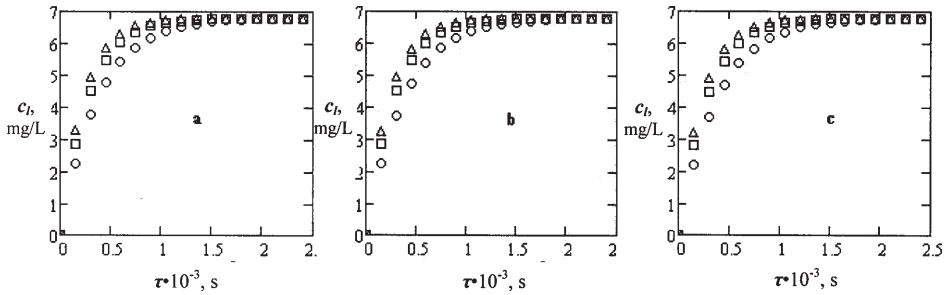

Fig. 6. Dynamics of water-BC oxygenation in Biostat Aplus bioreactor (V=1 L, t=30°C): a) n=800 rpm, c_{BC} =0.3%; b) n=800 rpm, c_{BC} =0.5%; c) n=800 rpm, c_{BC} =0.7% (o, □, Δ - as in fig. 4)

Table 4
DEPENDENCE OF *Sh* ON *Re* AND We_m FOR WATER-BC OXYGENATION IN BIOSTAT APLUS BIOREACTOR (t=30°C, D/d=3, H/d=2, h/d=0.6)

c_{BC}=0.3%			
Sh	$Re=1.095 \cdot 10^4$	$Re=2.19 \cdot 10^4$	$Re=3.503 \cdot 10^4$
$We_m=1.635 \cdot 10^{-5}$	$1.235 \cdot 10^3$	$2.611 \cdot 10^3$	$4.439 \cdot 10^3$
$We_m=3.371 \cdot 10^{-5}$	$1.687 \cdot 10^3$	$3.566 \cdot 10^3$	$6.064 \cdot 10^3$
$We_m=4.906 \cdot 10^{-5}$	$2.084 \cdot 10^3$	$4.271 \cdot 10^3$	$7.272 \cdot 10^3$
c_{BC}=0.5%			
Sh	$Re=9.684 \cdot 10^3$	$Re=1.937 \cdot 10^4$	$Re=3.099 \cdot 10^4$
$We_m=1.849 \cdot 10^{-5}$	$1.221 \cdot 10^3$	$2.582 \cdot 10^3$	$4.391 \cdot 10^3$
$We_m=3.697 \cdot 10^{-5}$	$1.668 \cdot 10^3$	$3.521 \cdot 10^3$	$5.998 \cdot 10^3$
$We_m=5.546 \cdot 10^{-5}$	$2.002 \cdot 10^3$	$4.224 \cdot 10^3$	$7.197 \cdot 10^3$
c_{BC}=0.7%			
Sh	$Re=8.835 \cdot 10^3$	$Re=1.767 \cdot 10^4$	$Re=2.827 \cdot 10^4$
$We_m=2.026 \cdot 10^{-5}$	$1.207 \cdot 10^3$	$2.551 \cdot 10^3$	$4.329 \cdot 10^3$
$We_m=4.053 \cdot 10^{-5}$	$1.649 \cdot 10^3$	$3.485 \cdot 10^3$	$5.927 \cdot 10^3$
$We_m=6.079 \cdot 10^{-5}$	$1.978 \cdot 10^3$	$4.174 \cdot 10^3$	$7.111 \cdot 10^3$

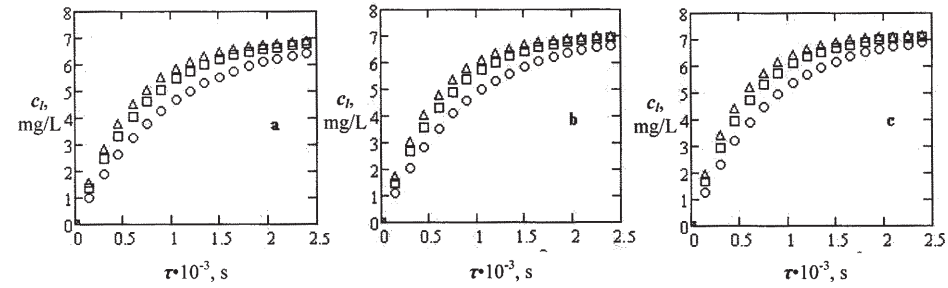

Fig. 7. Dynamics of distilled water-AC oxygenation in Biostat Aplus bioreactor (V=1 L, t=30°C): a) n=250 rpm, c_{AC} =0.3%; b) n=250 rpm, c_{AC} =1%; c) n=250 rpm, c_{AC} =3% (o, □, Δ - as in fig. 4).

Table 5
DEPENDENCE OF *Sh* ON *Re* AND We_m FOR WATER-AC OXYGENATION IN BIOSTAT APLUS BIOREACTOR (t=30°C, D/d=3, H/d=2, h/d=0.6)

c_{AC}=0.5%			
Sh	$Re=1.259 \cdot 10^4$	$Re=2.518 \cdot 10^4$	$Re=4.029 \cdot 10^4$
$We_m=1.422 \cdot 10^{-5}$	$1.750 \cdot 10^3$	$3.699 \cdot 10^3$	$6.291 \cdot 10^3$
$We_m=2.844 \cdot 10^{-5}$	$2.390 \cdot 10^3$	$5.054 \cdot 10^3$	$8.594 \cdot 10^3$
$We_m=4.266 \cdot 10^{-5}$	$2.868 \cdot 10^3$	$6.052 \cdot 10^3$	$10.03 \cdot 10^3$
c_{AC}=1%			
Sh	$Re=1.259 \cdot 10^4$	$Re=2.518 \cdot 10^4$	$Re=4.029 \cdot 10^4$
$We_m=1.422 \cdot 10^{-5}$	$1.917 \cdot 10^3$	$4.052 \cdot 10^3$	$6.99 \cdot 10^3$
$We_m=2.844 \cdot 10^{-5}$	$2.608 \cdot 10^3$	$5.561 \cdot 10^3$	$9.315 \cdot 10^3$
$We_m=4.266 \cdot 10^{-5}$	$3.131 \cdot 10^3$	$6.619 \cdot 10^3$	$11.29 \cdot 10^3$
c_{AC}=3%			
Sh	$Re=1.259 \cdot 10^4$	$Re=2.518 \cdot 10^4$	$Re=4.029 \cdot 10^4$
$We_m=1.422 \cdot 10^{-5}$	$2.167 \cdot 10^3$	$4.585 \cdot 10^3$	$7.693 \cdot 10^3$
$We_m=2.844 \cdot 10^{-5}$	$2.965 \cdot 10^3$	$6.257 \cdot 10^3$	$10.55 \cdot 10^3$
$We_m=4.266 \cdot 10^{-5}$	$3.491 \cdot 10^3$	$7.493 \cdot 10^3$	$12.67 \cdot 10^3$

water-BC oxygenation; ii) a slight increase in c_l^*as follows: c_l^*=7 mg/L for c_{AC}=0.3%, c_l^*=7.1 mg/L for c_{AC}=1%, and c_l^*=7.2 mg/L for c_{AC}=3%, respectively. Dependence of *Sh* number on *Re* and We_m numbers (table 5) has the same increasing trend as in the previous cases.

Experimental set 4 (aqueous phase: water-(AC-SO))

Using finely crushed particles of silicon oil impregnated activated carbon (AC-SO) as oxygen-vectors, values of oxygen equilibrium concentration less than 6.5 mg/L were obtained. Data presented in figure 8 and table 6 show a slight decrease in oxygen transfer rate with AC-SO concentration in water, $c_{AC\text{-}SO}$. Data summarized in Table 6, concerning the dependence of *Sh* number on *Re* and We_m numbers, emphasize lower values of *Sh* number comparative with those reported for activated carbon at similar levels of concentration.

Experimental set 5 (aqueous phase: water-MG)

The idea to test the magnetite (MG), Fe_3O_4, as oxygen-vector was based on its use as sorbent to remove charged species from water, e.g. the Sirofloc process employed for water decolourization [23]. Experimental curves depicted in figure 9 emphasize a faster saturation process at higher levels of MG concentration. An oxygen saturation degree of 90% is attained after 250 s for water containing 1% MG, whereas the same saturation degree is reached after 1000 s for water (fig. 4). Moreover, the equilibrium oxygen concentration in liquid phase, c_l*, slightly dependent on MG concentration in water, c_{MG}, has the following values at 30°C: 7.6 mg/L at c_{MG}=0.3%, 7.7 mg/L at c_{MG}=0.5%, and 7.8 mg/L for c_{MG}=1%, respectively. Characteristic data of experimental sets 1 and 5 reveal that the presence of MG powder at a concentration of 1% in water determines an increase in equilibrium oxygen concentration with 1 mg/L.

Data summarized in table 7 concerning the dependence of *Sh* on *Re* and We_m highlight a maximum value of *Sh* number of 31.64 . 10^3, about 4.3 times higher than that registered in the case of water oxygenation under the same operational conditions. Consequently, the magnetite powder can be used as an efficient oxygen-vector,

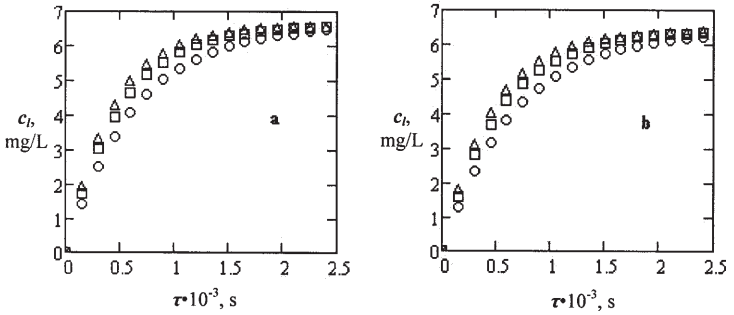

Fig. 8. Dynamics of water-(AC-SO) oxygenation in Biostat Aplus bioreactor (V=1 L, t=30°C):
a) n=500 rpm, $c_{AC\text{-}SO}$ =1%; b) n=500 rpm, $c_{AC\text{-}SO}$=2%
(o, □, Δ - as in fig. 4)

$c_{AC\text{-}SO}$=1%			
Sh	Re=1.253•10^4	Re=2.505•10^4	Re=4.090•10^4
We_m=1.429•10^{-5}	1.833•10^3	4.198•10^3	6.967•10^3
We_m=2.858•10^{-5}	2.337•10^3	5.239•10^3	8.766•10^3
We_m=4.287•10^{-5}	2.693•10^3	6.194•10^3	10.24•10^3
$c_{AC\text{-}SO}$=2%			
Sh	Re=1.253•10^4	Re=2.505•10^4	Re=4.090•10^4
We_m=1.429•10^{-5}	1.617•10^3	3.702•10^3	6.143•10^3
We_m=2.858•10^{-5}	2.061•10^3	4.496•10^3	7.732•10^3
We_m=4.287•10^{-5}	2.375•10^3	5.852•10^3	9.031•10^3

Table 6
DEPENDENCE OF *Sh* ON *Re* AND We_m FOR WATER-(AC-SO) OXYGENATION IN BIOSTAT APLUS BIOREACTOR (t=30°C, D/d=3, H/d=2, h/d=0.6)

contributing to a significant enhancement of oxygen mass transfer.

Experimental set 6 (aqueous phase: water-(BC-MG) composite)

All the four types of bacterial cellulose-magnetite (BC-MG) membranes synthesized in laboratory had a similar behaviour in testing as oxygen-vectors. Data depicted in figure 10, referring to any of these material types, reveal a faster oxygenation process at higher levels of BC-MG composite concentration in water, as in the case of water-MG system (fig. 9). The comparison between figures 9 and 10 shows a slightly higher rate of oxygen transfer in the presence of MG powder. Likewise, for MG powder or finely ground BC-MG composite, the concentration of dissolved oxygen at equilibrium ranging from 7.6 mg/L to 7.9 mg/L and is less influenced by the solid oxygen-vector concentration.

Experimental data presented in table 8 emphasize *Sh* number values similar to those obtained for magnetite powder (table 7) and about 4 times higher than results reported for bacterial cellulose, activated carbon, and silicon oil impregnated activated carbon (tables 4-6). Accordingly, the bacterial cellulose-magnetite (BC-MG) composite is an efficient oxygen-vector, which could have a good compatibility with many aerobic bacterial systems due to its matrix of bacterial cellulose.

Data correlation

According to Buckingham theorem in dimensional analysis, the oxygen mass transfer from air to liquid in stirred and aerated tank bioreactors can be described by relation (5) depending on similitude criteria *Sh*, *Re*, We_m as well as on geometric simplexes D/d, H/d, h/d [24]. As the values of geometric simplexes are constant, the relation (5) turns into correlation (6), where c, p, and q are constants.

$$f\left(Sh, \mathrm{Re}, We_m, \frac{D}{d}, \frac{H}{d}, \frac{h}{d}\right)=\mathrm{ct} \quad (5)$$

$$Sh = c\,\mathrm{Re}^{p}\,We_m^{\,q} \quad (6)$$

The values of c, p, and q were estimated by minimizing the expression (7), where Sh_i, Re_i, and We_{m_i} are experimental data summarized in tables 3-8 corresponding to each aqueous solution composition, i.e. type and concentration of oxygen-vector. The values of c, p, and q obtained by minimization are summarized in table 9. Values

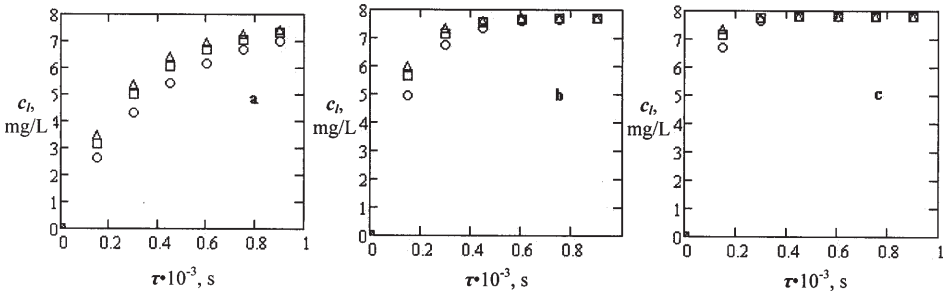

Fig. 9. Dynamics of water-MG oxygenation in Biostat Aplus bioreactor (V=1 L, t=30°C):
a) n=250 rpm, c_{MG}=0.3%; b) n=500 rpm, c_{MG}=0.5%; c) n=800 rpm, c_{MG}=1% (o, □, Δ - as in fig. 4).

c_{MG}=0.3%			
Sh	Re=1.242•10^4	Re=2.481•10^4	Re=3.969•10^4
We_m=1.441•10^{-5}	4.667•10^3	10.72•10^3	18.8410^3
We_m=2.887•10^{-5}	5.952•10^3	13.67•10^3	24.03•10^3
We_m=4.331•10^{-5}	6.855•10^3	15.75•10^3	27.76•10^3
c_{MG}=0.5%			
Sh	Re=1.248•10^4	Re=2.496•10^4	Re=3.994•10^4
We_m=1.434•10^{-5}	5.005•10^3	11.49•10^3	20.1910^3
We_m=2.869•10^{-5}	6.375•10^3	14.64•10^3	25.74•10^3
We_m=4.303•10^{-5}	7.345•10^3	16.87•10^3	29.66•10^3
c_{MG}=1%			
Sh	Re=1.222•10^4	Re=2.445•10^4	Re=3.911•10^4
We_m=1.465•10^{-5}	5.333•10^3	12.25•10^3	21.54•10^3
We_m=2.929•10^{-5}	6.801•10^3	15.62•10^3	27.44•10^3
We_m=4.394•10^{-5}	7.835•10^3	18.01•10^3	31.64•10^3

Table 7
DEPENDENCE OF *Sh* ON *Re* AND We_m FOR WATER-MG OXYGENATION IN BIOSTAT APLUSBIOREACTOR (t=30°C, D/d=3, H/d=2, h/d=0.6)

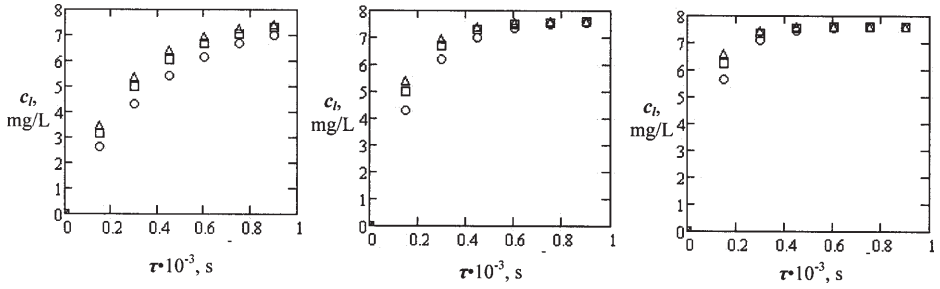

Fig. 10. Dynamics of water-(BC-MG) composite oxygenation in Biostat Aplus bioreactor (V=1 L, t=30°C): a) n=250 rpm, $c_{BC\text{-}MG}$=0.3%; b) n=500 rpm, $c_{BC\text{-}MG}$=0.5%; c) n=800 rpm, $c_{BC\text{-}MG}$=0.7% (o, □, Δ - as in fig. 4).

$c_{BC\text{-}MG}$=0.3%			
Sh	Re=1.247•10^4	Re=2.493•10^4	Re=3.989•10^4
We_m=1.436•10^{-5}	4.167•10^3	9.58•10^3	16.4410^3
We_m=2.875•10^{-5}	5.313•10^3	12.61•10^3	21.83•10^3
We_m=4.309•10^{-5}	6.121•10^3	14.05•10^3	24.82•10^3
$c_{BC\text{-}MG}$=0.5%			
Sh	Re=1.234•10^4	Re=2.469•10^4	Re=3.952•10^4
We_m=1.451•10^{-5}	4.511•10^3	10.31•10^3	18.1710^3
We_m=2.901•10^{-5}	5.737•10^3	13.18•10^3	23.17•10^3
We_m=4.351•10^{-5}	6.611•10^3	15.18•10^3	26.69•10^3
$c_{BC\text{-}MG}$=0.7%			
Sh	Re=1.221•10^4	Re=2.441•10^4	Re=3.909•10^4
We_m=1.465•10^{-5}	4.833•10^3	12.55•10^3	19.52•10^3
We_m=2.929•10^{-5}	6.162•10^3	14.16•10^3	24.88•10^3
We_m=4.391•10^{-5}	7.103•10^3	16.31•10^3	28.57•10^3

Table 8
DEPENDENCE OF *Sh* ON *Re* AND We_m FOR WATER-(BC-MG) COMPOSITE OXYGENATION IN BIOSTAT APLUS BIOREACTOR (t=30°C, D/d=3, H/d=2, h/d=0.6)

of *Re* number power, p, ranging from 1.19 to 1.24 were obtained, according to manifold correlations in the related literature.

$$F(c,p,q)=\sum_{i=1}^{9}\left(Sh_i - c\,\mathrm{Re}_i^{\,p}\,We_{m_i}^{q}\right)^2 \qquad (7)$$

For MG and BC-MG composite, a term highlighting the influence of oxygen-vector concentration, i.e. $c_{ov}/c_{ov,max}$, was added in the correlation (6), resulting the expression (8), where c', α, and β are constants and $c_{ov,max}$ is the maximal concentration of solid oxygen-vector used in experiments. For a proper identification of α and β parameters, two sets of 9 experiments were performed at a concentration of MG and BC-MG composite, respectively, of 0.15%. The correlations (9) and (10), whose coefficients were estimated based on experimental data and results predicted by relation (8), reveal a similar behaviour of MG and BC-MG composite as oxygen-vectors.

Experimental and predicted values of *Sh* number shown in figure 11 emphasize an accurate identification of characteristic parameters of correlations (6) and (8). Furthermore, the data in Figure 11 highlight the magnitude of *Sh* number. Accordingly, comparing characteristic *Sh* number of water oxygenation with those obtained for aqueous solution containing MG or BC-MG composite,

No.	Aqueous solution	c_l^* (mg/L)	Particular form of relation (6)
1	Water	6.8	$Sh = 1.41\mathrm{Re}^{1.194}\,We_m^{0.407}$
2	Water with 0.3% BC	6.8	$Sh = 0.778\mathrm{Re}^{1.213}\,We_m^{0.37}$
3	Water with 0.5% BC	6.8	$Sh = 0.778\mathrm{Re}^{1.213}\,We_m^{0.37}$
4	Water with 0.7% BC	6.8	$Sh = 0.781\mathrm{Re}^{1.212}\,We_m^{0.37}$
5	Water with 0.5% AC	7.1	$Sh = 1.29\mathrm{Re}^{1.236}\,We_m^{0.407}$
6	Water with 1% AC	7.2	$Sh = 1.165\mathrm{Re}^{1.241}\,We_m^{0.385}$
7	Water with 3% AC	7.3	$Sh = 0.925\mathrm{Re}^{1.284}\,We_m^{0.403}$
8	Water with 1% AC-SO	6.5	$Sh = 0.713\mathrm{Re}^{1.19}\,We_m^{0.33}$
9	Water with 2% AC-SO	6.5	$Sh = 0.733\mathrm{Re}^{1.19}\,We_m^{32}$
10	Water with 0.3% MG	7.7	$Sh = 3.296\mathrm{Re}^{1.19}\,We_m^{0.352}$
11	Water with 0.5% MG	7.8	$Sh = 3.386\mathrm{Re}^{1.19}\,We_m^{0.35}$
12	Water with 1% MG	7.8	$Sh = 3.423\mathrm{Re}^{1.19}\,We_m^{0.348}$
13	Water with 0.3% BC-MG	7.6	$Sh = 2.689\mathrm{Re}^{1.192}\,We_m^{0.348}$
14	Water with 0.5% BC-MG	7.7	$Sh = 2.997\mathrm{Re}^{1.193}\,We_m^{0.351}$
15	Water with 0.7% BC-MG	7.8	$Sh = 3.14\mathrm{Re}^{1.196}\,We_m^{0.352}$

Table 9
VALUES OF c, p, AND q DEPENDING ON AQUEOUS SOLUTION COMPOSITION IN BIOSTAT APLUS BIOREACTOR (t=30°C, D/d=3, H/d=2, h/d=0.6)

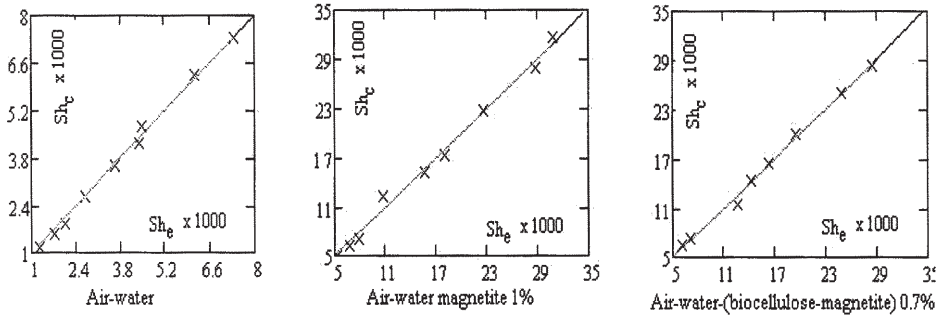

Fig. 11. Experimental (e) and predicted (c) Sherwood number values

respectively, values of about four times lower are observed for water.

$$Sh = c'\left(1+\alpha\left(\frac{c_{ov}}{c_{ov,\max}}\right)^{\beta}\right)\mathrm{Re}^{p}\,We_m^{\,q} \quad (8)$$

$$Sh = 1.14\left(1+2.423\left(\frac{c_{MG}}{c_{MG,\max}}\right)^{0.11}\right)\mathrm{Re}^{1.19}\,We_m^{\,0.37} \quad (9)$$

$$Sh = 1.14\left(1+2.125\left(\frac{c_{BC-MG}}{c_{BC-MG,\max}}\right)^{0.11}\right)\mathrm{Re}^{1.19}\,We_m^{\,0.37} \quad (10)$$

Conclusions

In order to enhance the oxygen transfer for mechanically stirred and aerated bioreactors, fine particles of activated carbon, silicon oil impregnated activated carbon, bacterial cellulose, magnetite, and bacterial cellulose-magnetite composite were used as solid oxygen-vectors. Preparation procedure and structural characterization of bacterial cellulose-magnetite composite were detailed. The experiments were performed in a Biostat Aplus Sartorius bioreactor equipped with a six-blade disk impeller, vertical baffles, and an air micro-sparger system for a proper homogenization and aeration of liquid phase.

The paper aimed at establishing the dependence of oxygen volumetric mass transfer coefficient, k_la, on liquid phase composition, stirring and aeration conditions. A dynamic method based on oxygen degassing and re-aeration of liquid phase, consisting of water or aqueous solutions containing various amounts of solid oxygen-vector, was selected for experimental determination of k_la. 153 of curves characterizing the dynamics of liquid phase oxygenation were obtained and used for k_la identification. An important influence of stirring speed and aeration flow rate, expressed as dynamic air intake, on the volumetric mass transfer coefficient, k_la, was assessed. Moreover, the presence of magnetite and bacterial cellulose-magnetite composite determined a significant enhancement of oxygen mass transfer.

The experimental data were valorised in terms of k_la dependence of stirring and aeration conditions, i.e.$Sh = c\mathrm{Re}^{p}\mathrm{We}_m^{\,q}$. Values of Reynolds number power, p, between 1.19 and 1.25 were obtained, according to the results reported in the related literature. Additionally, for magnetite and bacterial cellulose-magnetite composite, the effect of oxygen-vector concentration in water, c_{ov}, was evaluated. A very good agreement between experimental and predicted values of *Sh* number was obtained.

Aknowledgement: POSDRU Project 76909 support is gratefully acknowledged.

References

1. DUNN, I.J., HEINZLE, E., INGHAM, J., PRENOZIL, J.E., Biological reaction engineering: Principles, applications and modelling with PC simulation, VCH, Weinheim, 1992
2. JU, L.K., SUNDARARAJAN, A., Biotechnol. Bioeng, **40**, 1992, p. 1343
3. RUTHIYA, K.C., van der SCHAAF, J., KUSTER, B.F.M., SCHOUTEN, J.C., Chem. Eng. J., **96**, 2003, p. 55
4. CLARKE, K.G., CORREIA, L.D.C., Biochem. Eng. J., **39**, 2008, p. 405
5. GARCIA-OCHOA, F., GOMEZ, E., Biotech. Adv., **27**, 2009, p. 153
6. LINEK, V., VACEK, V., Chem. Eng. Technol., **11**, 1981, p. 249
7. STOENICĂ, M., LAVRIC, V., Rev. Chim. (Bucharest), **61**, no. 4, 2010, p. 407
8. ENE, M., JIPA, I., GHEORGHE M., STOICA, A., STROESCU, M., Rev. Chim. (Bucharest), **62**, no. 2, 2011, p. 227
9. MOUCHA, T., REJL, J.F., KORDAC, M., LABIK, L., Biochem. Eng. J., **69**, 2012, p. 17
10. MARTÍN, M., MONTES, F.J., GALÁN, M.A., Chem. Eng. Sci., **65**, 2010, p. 3814
11. JAMNONGWONG, M., LOUBIERE, K., DIETRICH, N., HÉBRARD, G., Chem. Eng. J., **165**, 2010, p. 758
12. CALUSARU, I.M., BĂRAN, N., PĂTULEA, A., Adv. Mater. Res., **538-541**, 2012, p. 2304
13. DUMONT, E., ANDRČS, Y., Le CLOIREC, P., Biochem. Eng. J., **30**, 2006, p. 245
14. LEUNG, R., PONCELET, D., NEUFELD, R.J., J. Chem. Technol. Biot., **68**, 1997, p. 37
15. NARTA, U., ROY, S., KANWAR, S.S., AZMI, W., Bioresour. Technol., **102**, 2011, p. 2083
16. SAUID, S.M., MURTHY, V.V.P.S., Journal of Applied Sciences, **10**, 2010, p. 2745
17. ZHAO, S., KUTTUVA, S.G., JU, L.K., Bioprocess Eng., **20**, 1999, p. 313
18. PULIDO-MAYORAL, N., GALINDO, E., Biotechnol. Progr., **20**, no. 5, 2004, p. 1608
19. ALPER, E., WICHTENDAHLET, B., DECKWER, W.D., Chem. Eng. Sci., **35**, 1980, p. 217
20. LU, W.M., HSU, R.C., CHOU, H.S., Journal Chin. I. Chemical Engineering, **24**, 1993, p. 31
21. DOBRE, T., STOICA, A., PÂRVULESCU, O.C., STROESCU, M., IAVORSCHI, G., Rev. Chim. (Bucharest), **59**, no. 5, 2008, p. 590
22. DOBRE, L.M., STOICA-GUZUN, A., J. Biobased Mater. Bio., **7**, 2013, p. 157
23. DIXON, D. R., Water Supply, **9**, 1991, p. 33
24. DOBRE, T., SANCHEZ MARCANO, J., Chemical engineering - modelling, simulation and similitude, Wiley VCH, 2007, p. 466

Manuscript received; 21.10.2013